Proceedings of the Conference on Computational Engineering and Science JSCES
Vol. 30, Jun. 2025

Data-driven topology design with image fragmented learning: Application to turbulent heat transfer problems

Yusibo Yang [1] , Kentaro Yaji [2] and Kikuo Fujita [3]

[1]Graduate School of Engineering, The University of Osaka, 565-0871, Suita, Japan. E-mail: yang@syd.mech.eng.osaka-u.ac.jp
[2]Ph.D. Graduate School of Engineering, The University of Osaka, 565-0871, Suita, Japan. E-mail: yaji@mech.eng.osaka-u.ac.jp
[3]Dr.Eng. Graduate School of Engineering, The University of Osaka, 565-0871, Suita, Japan. E-mail: fujita@mech.eng.osaka-u.ac.jp

Original data-driven topology design methods often experience a decline in training effectiveness as input dimensionality increases, which limits their applicability to high-dimensional tasks. To overcome the limitation, we introduce a DDTD framework enhanced by image fragmented learning (IFL). In the IFL-DDTD framework, large input images are segmented into smaller fragments, each learned independently using a module from a pre-trained pix2pix model. pix2pix consists of a downscale module and a regeneration module, which together allow for seamless transitions between low and high dimensional representations during the design process. We demonstrate the efficacy of IFL-DDTD by applying it to a turbulent heat transfer problem. Our results demonstrate that the proposed framework effectively accommodates high-dimensional design variables and significantly outperforms original DDTD methods.

Key Words : *Data-driven topology design, turbulent heat transfer, image translation*

1. Introduction

Topology optimization (TO) is an efficient method for solving design problems and offers a high degree of design freedom, which facilitates the development of optimal structures [1]. However, gradient-based TO often falls into local solutions, which limits its effectiveness in solving multi-objective optimization problems.

Data-driven topology design (DDTD) has emerged as a sensitivity-free method capable of generating diverse material distributions from a small set of latent variables, which is suitable for strongly nonlinear multi-objective problems [2,3,4]. Despite recent advances in DDTD, the generative approach encounters computational limitations when the number of design variables becomes excessively large. Original DDTD methods typically compress the design space into low-dimensional latent representations to improve computational efficiency. However, the compression constrains solution diversity and degrades the quality of the generated designs. This limitation makes it particularly challenging to apply DDTD to high-dimensional problems [5].

In this paper, we propose an enhanced DDTD framework called IFL-DDTD (DDTD with image fragmentated learning). The framework integrates an image translation neural network [6] into the original DDTD process. IFL process represents the design variables as pixel-based distributions and processing them through neural network-driven image transformation techniques, the proposed framework enables efficient dimensional compression and reconstruction of high-dimensional design data.

The proposed framework is applied to a two-dimensional turbulent heat transfer design problem characterized by strong nonlinearities and high-dimensional design variables, which cannot be solved by original DDTD methods. To address this problem , the design domain is decomposed into smaller structural fragments, and neural network tiling is employed. This strategy enables the IFL framework to effectively handle high-dimensional optimization tasks while preserving intricate structural features. As a result, the proposed framework successfully generates diverse, high-resolution structural designs.

The remainder of this paper is structured as follows. **Section 2** presents the proposed method and shows the IFL-DDTD framework. **Section 3** introduces the turbulent heat transfer design problem and details the application of the proposed framework. **Section 4** provides numerical results and compares the performance of the results from proposed framework with the results of original framework. Finally, **Section 5** concludes the paper with a summary of the main findings and discusses potential directions for further work.

2. Proposed framework

(1) Basic concept

Fig. 1 illustrates the flowchart of the proposed IFL-DDTD framework, which extends the original multifidelity DDTD design process. The initial steps include low-fidelity optimization, high-fidelity evaluation, and elite solution selection. These procedures are consistent with those used in original DDTD. The core contribution of our framework lies in the integration of the IFL process. In this process, a downscale module is introduced before the variational autoencoder (VAE) to compress the high-dimensional data into a low-dimensional representation.

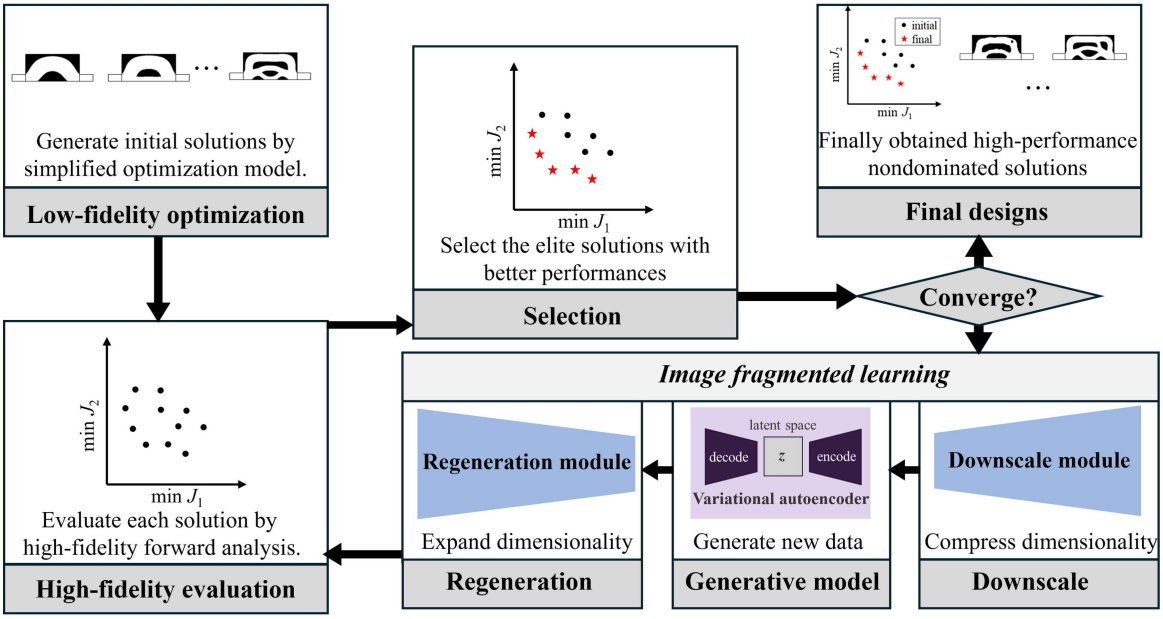

Fig. 1 Flowchart illustrating the data process of IFL-DDTD

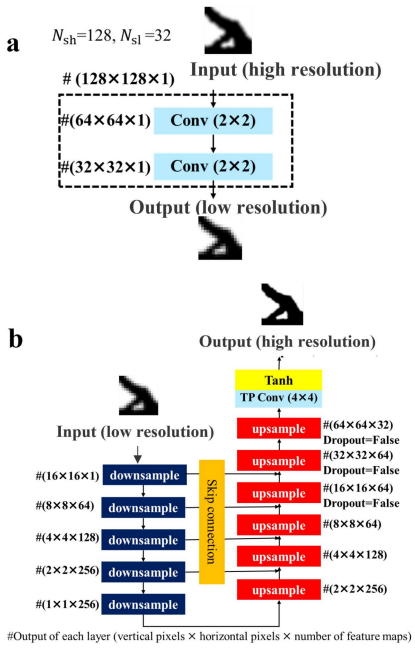

Fig. 2 Modules obtained by splitting the proposed neural network for dimensionality transformation. a: downscale module, b: regeneration module

After new samples are generated by the VAE, a regeneration module is applied to reconstruct the data back to its original high-dimensional form. This architecture enables efficient dimensional compression, generation of new low-dimensional samples through VAE learning, and accurate reconstruction of high-dimensional design data.

(2) Construction of IFL-DDTD

To construct the dimensional transformation modules, we adopt the pix2pix neural network, a conditional generative adversarial network (cGAN) that incorporates resolution downscaling and upscaling components in its architecture [6]. These architectural features are well aligned with our objective of compressing high-dimensional design variables and subsequently reconstructing them.

For addressing the high-dimensional nature of this design problem, we employ a pix2pix network with an input resolution of $N_{\mathrm{sh}} = 128$. This network is divided into two distinct modules: a downscale module responsible for dimensionality reduction, and a regeneration module that restores the original dimensionality. Based on our preliminary experiments, we selected N_{sl} as the target resolution, which achieves a favorable trade-off between compression

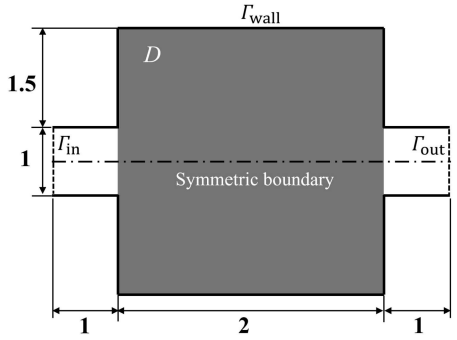

Fig. 3 Design domain and boundary conditions of heat transfer

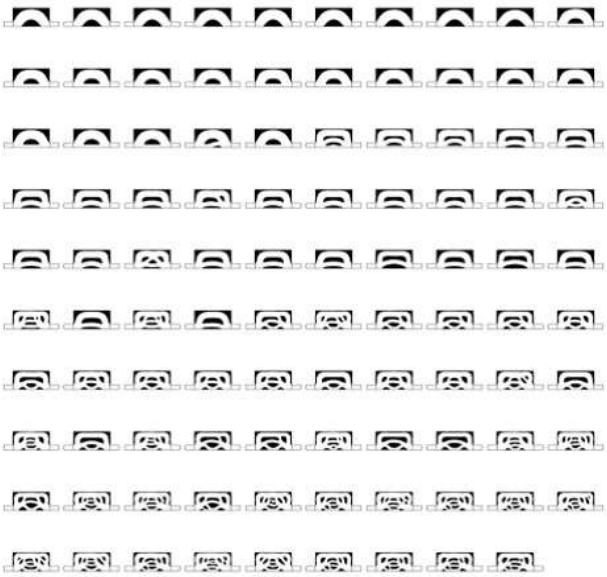

Fig. 4 99 initial data obtained through TO of laminar heat transfer design

and fidelity. This configuration ensures that reconstructed images closely match the originals without noticeable segmentation artifacts. The architectures of the trained downscale and regeneration modules are illustrated in **Fig. 2**. Through this design, the practical IFL-DDTD is successfully established.

3. Turbulent heat transfer design

(1) Problem setting

In this section, we apply the IFL-DDTD framework to solve a strongly nonlinear design problem. We consider a two-dimensional turbulent heat transfer problem with the design domain and corresponding boundary conditions shown in **Fig. 3**. The design variable field is defined as $\gamma = 0$ for solid regions and $\gamma = 1$ for fluid regions.

The physical behavior of the system is governed by fluid velocity $\mathbf{v}$, pressure p, and temperature T. To model turbulent flow, we adopt the Reynolds Averaged Navier–Stokes (RANS) equations with the standard k–ϵ turbulence model [7], where k denotes turbulent kinetic energy and ϵ denotes its dissipation rate. The governing equations are as follows:

$$\begin{aligned}
\nabla \cdot \mathbf{v} =& 0 \\
(\mathbf{v} \cdot \nabla)\mathbf{v} =& -\nabla p + \nabla(\mu + \mu_t)(\nabla \mathbf{v} + (\nabla \mathbf{v})^T) \\
& - \alpha_\gamma \mathbf{v} \\
(\mathbf{v} \cdot \nabla)k =& \nabla \left[\left(\mu + \frac{\mu_t}{\sigma_k} \right) \nabla k \right] + P_k - \epsilon \\
(\mathbf{v} \cdot \nabla)\epsilon =& \nabla \left[\left(\mu + \frac{\mu_t}{\sigma_\epsilon} \right) \nabla \epsilon \right] \\
& + C_{\epsilon 1} \frac{\epsilon}{k} P_k - C_{\epsilon 2} \frac{\epsilon^2}{k} \\
\mathbf{v} \cdot \nabla T =& \nabla \cdot \left(\left(\frac{\mu}{Pr} + \frac{\mu_t}{Pr_t} \right) \nabla T \right)
\end{aligned} \tag{1}$$

where μ represents the kinematic viscosity, which is inversely scaled by the Reynolds number Re under the characteristic speed and length are one. The turbulent eddy viscosity μ_t is given by $\mu_t = C_\mu \frac{k^2}{\epsilon}$, where k and ϵ represent the turbulent kinetic energy and its dissipation rate, respectively.

The design-dependent parameter α_γ is defined as 0 in fluid regions and as the inverse permeability α in solid regions. The term P_k represents the production of turbulent kinetic energy caused by velocity gradients and is expressed as:

$$P_k = \mu_t \left[\nabla \mathbf{v} : \left(\nabla \mathbf{v} + (\nabla \mathbf{v})^T \right) \right] \tag{2}$$

In addition, Pr denotes the Prandtl number, and Pr_t is the turbulent Prandtl number, both critical for thermal

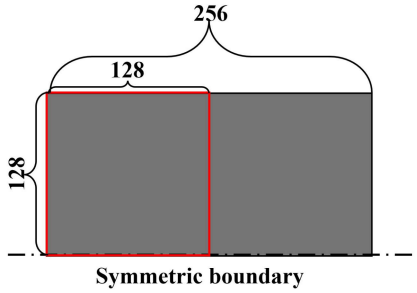

Fig. 5 The symmetric heat transfer mesh is segmented into square fragments, each with a size of 128×128

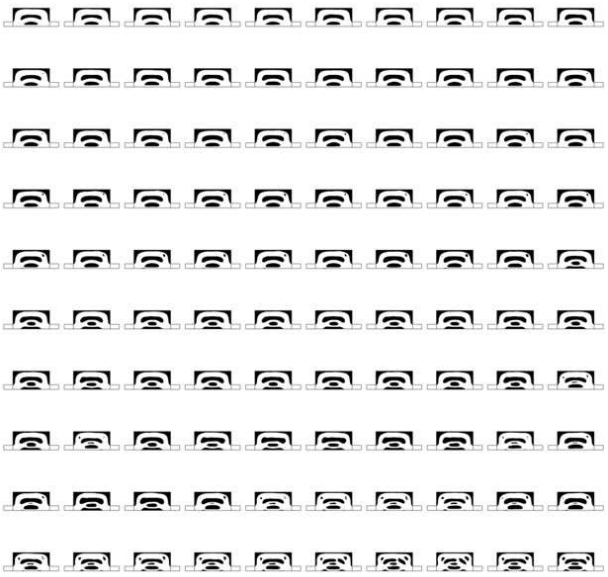

Fig. 6 Obtained 100 samples of optimized turbulent heat transfer by 400 iterations

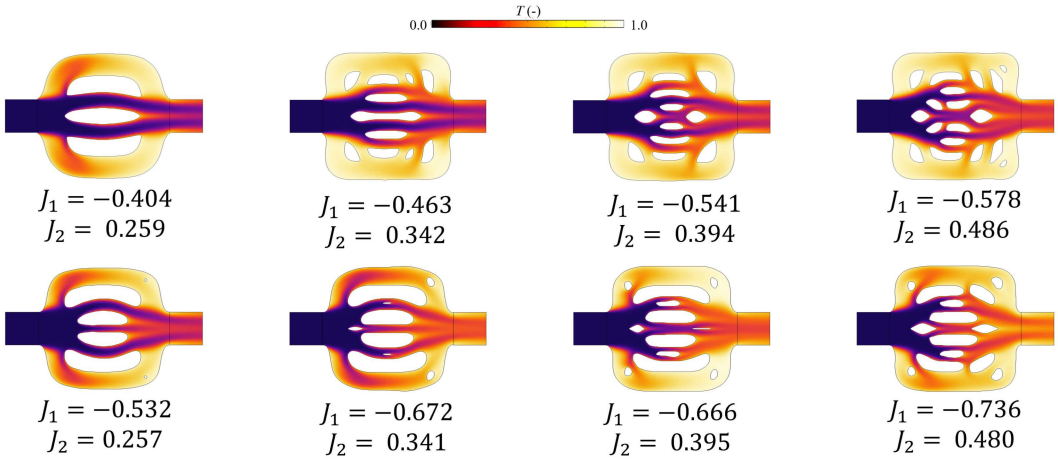

Fig. 7 Comparison of temperature distribution between initial (top row) and optimized (bottom row) flow channels under similar pressure dissipation conditions

transport calculations. The empirical constants used in the turbulence model are as follows: $C_\mu = 0.09$, $C_{\epsilon 1} = 1.44$, $C_{\epsilon 2} = 1.92$, $\sigma_k = 1.0$, and $\sigma_\epsilon = 1.3$.

The boundary conditions applied at the inlet (Γ_{in}), outlet (Γ_{out}), walls (Γ_{wall}) and heated surface (Γ_{heated}) are described as follows:

$$\begin{aligned} \mathbf{v} = -\mathbf{n}, \quad T = 0 \quad & \text{on } \Gamma_{\text{in}} \\ p = 0, \quad \mathbf{n} \cdot \nabla T = 0 \quad & \text{on } \Gamma_{\text{out}} \\ \mathbf{v} = \mathbf{0}, \quad \mathbf{n} \cdot \nabla T = 0 \quad & \text{on } \Gamma_{\text{wall}} \\ T = 1 \quad & \text{on } \Gamma_{\text{heated}} \end{aligned} \tag{3}$$

where $\mathbf{n}$ is the outward unit normal vector. The thermal boundary condition $T = 1$ imposed on Γ_{heated} defines the region responsible for heat transfer into the fluid.

(2) High-fidelity evaluation

This optimization problem aims to achieve two goals. The first is to maximize the average outlet temperature T_{out}, which reflects the efficiency of heat transfer. The second is to minimize the inlet pressure p_{in}, which contributes to reducing pressure losses. These objectives are mathematically expressed as follows.

$$\begin{aligned} \text{Minimize} \quad J_1 &= -T_{\text{out}} = -\frac{\int_{\Gamma_{\text{out}}} T \mathrm{d}\Gamma}{|\Gamma_{\text{out}}|} \\ J_2 &= p_{\text{in}} = \frac{\int_{\Gamma_{\text{in}}} p \mathrm{d}\Gamma}{|\Gamma_{\text{in}}|} \end{aligned} \tag{4}$$

The two objective functions are applied during the high-fidelity evaluation phase [8], which is conducted under high Reynolds number conditions to simulate turbulent flow. In this stage, the two objective functions, outlet temperature and inlet pressure, are directly computed via finite element simulation. These quantitative evaluations serve as the basis for selecting superior design candidates.

This strategy enables effective handling of strongly nonlinear turbulent phenomena. By decoupling the surrogate model from the final evaluation, the framework avoids reliance on gradient-based TO methods, which often fail to converge in such complex, non-convex design spaces.

(3) Low-fidelity approximation and initial designs

Due to the complexity inherent in turbulent optimization, initial material distributions are generated using a simplified low-fidelity model based on laminar flow assumptions. The design domain is discretized into 65,536 square elements, yielding high-dimensional initial solutions at reduced cost. As illustrated in **Fig. 4**, 99 initial designs are obtained via topology optimization under varying laminar Reynolds number conditions.

At this high-dimensional scale, generative models employed in original DDTD frameworks fail to effectively handle the design space, as discussed in **Section 1**. This limitation prevents the original DDTD from generating viable solutions. Therefore, to address this challenge, we applied IFL-DDTD framework capable of accommodating such high-dimensional inputs.

(4) Implementation details

To enable proposed framework to effectively address the high-dimensional design problem, we apply the proposed modules to process the symmetric discretized design domain, as illustrated in **Fig. 5**. Specifically, the downscale module is employed to reduce the dimensionality of the original high-resolution grid of size 256×128. The domain is first partitioned into two subdomains of 128×128, and each subdomain is subsequently downsampled to a 32×32 representation. As a result, the overall input is transformed into a compact low-dimensional dataset. This resolution is well-suited for training the VAE, enabling it to effectively capture the underlying design features.

Using the integrated transformation modules, the input dimensionality is reduced from 65,536 to 4,096, and can later be reconstructed to its original resolution via the

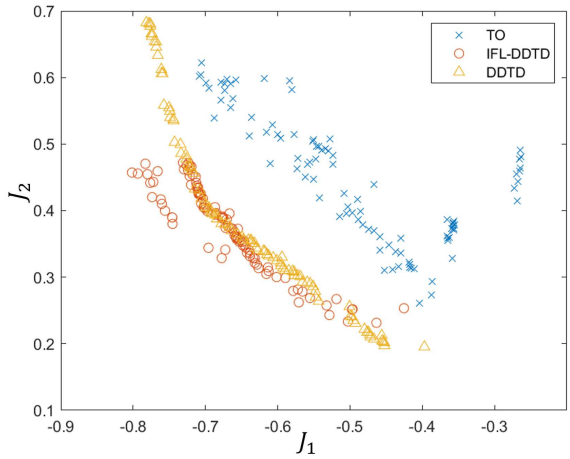

Fig. 8 Comparison of objective spaces among TO, DDTD, and the proposed IFL-DDTD

regeneration module. This two-stage transformation facilitates efficient exploration of high-dimensional design spaces and overcomes the scalability limitations inherent in original DDTD methods.

4. Results and discussion

(1) Flow configurations and simulation results

The proposed dimensional transformation framework was successfully implemented. Convergence of the optimization process was achieved after 400 iterations, with the elite solutions illustrated in **Fig. 6**. In comparison to the initial dataset, the resulting structures exhibit a marked reduction in geometric complexity, enhanced structural stability, and the emergence of consistent characteristic features. To quantitatively assess the performance of the generated flow channels, high-fidelity simulations were conducted to evaluate their thermal and fluid flow characteristics, as presented in **Fig. 7**.

The optimized flow channels consistently demonstrate enhanced thermal performance, achieving higher heat transfer efficiency while maintaining low-pressure losses. These results underscore the effectiveness of the proposed framework in balancing thermal and fluid dynamic objectives.

(2) Comparison of objective performance

To evaluate the effectiveness of the proposed method, we compared it against the original DDTD framework operating at a dimensionality of 8,192, which is considered a computationally efficient setting for original generative models. After 400 iterations, the resulting objective spaces from IFL-DDTD (our proposed framework), original DDTD, and the initial topology optimization (TO) dataset were compared, as shown in **Fig. 8**.

The results clearly indicate that the IFL-DDTD framework achieves superior optimization performance compared to the original DDTD framework. Not only does IFL-DDTD achieve better objective values in both heat transfer and pressure loss metrics, but it also enables stable and efficient computation in significantly higher-dimensional design spaces. This highlights the scalability and enhanced optimization capability of the proposed framework, which effectively overcomes the dimensional limitations faced by original DDTD methods.

5. Conclusion

In this study, we proposed an enhanced data-driven topology design (DDTD) framework using image fragmented learning (IFL) to address high-dimensional, multi-objective optimization in turbulent heat transfer problems. By integrating a pix2pix-based image translation network with a generative model, IFL enables effective dimensional compression and reconstruction. Applied to turbulent heat transfer, the proposed method produced optimized flow configurations that outperform conventional DDTD in both performance and scalability. Future work will explore its application to more complex problems and investigate advanced neural architectures beyond pix2pix to further improve design quality.

ACKNOWLEDGMENT This work was supported by JSPS KAKENHI (Grant No. 23H03799).

REFERENCES

[1] Bendsøe, M.P., and Kikuchi, N., Generating optimal topologies in structural design using a homogenization method, *Comput. Meth. Appl. Mech. Engng*, 71(2): 197-224, 1988.

[2] Yamasaki, S., Yaji, K., and Fujita, K., Data-driven topology design using a deep generative model, *Struct. Multidiscip. Optim*, pp.1401-1420, 2021.

[3] Kato, M., Kii, T., Yaji, K., et al., Maximum stress minimization via data-driven multifidelity topology design, 2024.

[4] Kii, T., Yaji, K., Fujita, K., et al., Latent crossover for data-driven multifidelity topology design, *J. Mech. Des*, 146(5): 051713, 2024.

[5] Yang, J., Yaji, K., and Yamasaki, S., Data-driven topology design based on principal component analysis for 3D structural design problems, 2024.

[6] Isola, P., Zhu, J.Y., Zhou, T.H., et al., Image-to-image translation with conditional adversarial networks, *In: Proceedings of the IEEE Conference on Computer Vision and Pattern Recognition (CVPR)*, 2017.

[7] Yaji, K., Yamasaki, S., and Fujita, K., Data-driven multi-fidelity topology design using a deep generative model: Application to forced convection heat transfer problems, *Comput. Meth. Appl. Mech. Engng*, 388:114284, 2022.

[8] Yaji, K., Yamasaki, S., and Fujita, K., Multifidelity design guided by topology optimization. *Struct. Multidiscip. Optim*, 42(6):939-953, 2020.